Inorg. Chem. **2004**, *43*, 895–904

Characterization of the Thermally Induced Topochemical Solid-State Transformation of $NH_4[N(CN)_2]$ into $NCN{=}C(NH_2)_2$ by Means of X-ray and Neutron Diffraction as Well as Raman and Solid-State NMR Spectroscopy

Bettina V. Lotsch, Jürgen Senker, and Wolfgang Schnick*

Department Chemie, Ludwig-Maximilians-Universität München, Butenandtstrasse 5-13 (D), D-81377 München, Germany

Received August 19, 2003

The mechanism of the solid–solid transformation of $NH_4[N(CN)_2]$ into $NCN{=}C(NH_2)_2$, which represents the isolobal analogue of Wöhler's historic conversion of ammonium cyanate into urea, has been investigated by temperature-dependent single-crystal and powder X-ray diffraction, neutron powder diffraction, and Raman and solid-state NMR spectroscopy as well as thermoanalytical measurements. The transformation of the ionic dicyanamide into its molecular isomer upon controlled thermal treatment was found to proceed topochemically in the solid state with little molecular motion, giving rise to a single-crystal to single-crystal transformation which manifests itself by a defined metric relation between the unit cells of the two isomers. The exothermic phase transition is thermally activated and was observed to commence at temperatures ≥ 80 °C. The pronounced temperature dependence of the onset of the transformation may be assessed as an indication for the metastability of ammonium dicyanamide at elevated temperatures. Thermal analyses reveal a decrease in the reaction enthalpy (56–13 kJ mol^{-1}) at higher heating rates and an average mass loss of 10% gaseous ammonia. Evidence was found for crucial mechanistic steps of the transformation, which is likely to proceed via proton transfer from the ammonium ion to one of the terminal nitrogen atoms of the anion. The protonation is followed by nucleophilic attack of the in situ generated ammonia at the electrophilic nitrile carbon. The proposed mechanistic pathway is based on the results of combined Raman and solid-state NMR spectroscopic as well as neutron powder diffraction measurements.

Introduction

Over the past decade, considerable research efforts have been centered on novel molecular routes to covalently linked C_xN_y extended solids. A particularly intriguing feature of carbon nitride chemistry is the prospect of outstanding material properties predicted for the binary carbon nitride C_3N_4,[1−3] which may be obtained by high-pressure treatment of graphitic carbon nitride phases (g-C_3N_4). The latter have attracted concentrated attention due to their hitherto unknown structural properties. Several synthetic approaches to 2-D and 3-D C_3N_4 structures based on the triamino tris-*s*-triazine and *s*-triazine units have been reported [4−16] and complemented by detailed theoretical calculations. On this background, structural models have been proposed for the graphitic phases of C_3N_4; however, their existence and preference of formation in terms of energetic stability is still a point at issue. Although the necessity to learn about the composition and metrics as

* To whom correspondence should be addressed. E-mail: wolfgang.schnick@uni-muenchen.de. Tel.: +49/89-2180-77436. Fax: +49/89-2180-77440.

(1) Liu, A. Y.; Cohen, M. L. *Science* **1989**, *245*, 841.
(2) Niu, C.; Lu, Y. Z.; Lieber, C. M. *Science* **1993**, *261*, 334.
(3) Fang, P. H. J. *Mater. Sci. Lett.* **1995**, *14*, 536.
(4) Zhang, Z.; Leinenweber, K.; Bauer, M.; Garvie, L. A. J.; McMillan, P. F.; Wolf, G. H. *J. Am. Chem. Soc.* **2001**, *123*, 7788.
(5) Komatsu, T.; Nakamura, T. *J. Mater. Chem.* **2001**, *11*, 474.
(6) Gillan, E. G. *Chem. Mater.* **2000**, *12*, 3906.
(7) Khabashesku, V. N.; Zimmerman, J. L.; Margrave, J. L. *Chem. Mater.* **2000**, *12*, 3264.
(8) Kawaguchi, M. *Chem. Mater.* **1995**, *7*, 257.
(9) Hosmane, R. S.; Rossman, M. A.; Leonard, N. J. *J. Am. Chem. Soc.* **1982**, *104*, 5497.
(10) Shahbaz, M.; Urano, S.; LeBreton, P. R.; Rossman, M. A.; Hosmane, R. S.; Leonard, N. J. *J. Am. Chem. Soc.* **1984**, *106*, 2805.
(11) Kroke, E.; Schwarz, M.; Horath-Bordon, E.; Kroll, P.; Noll, B.; Norman, A. D. *New J. Chem.* **2002**, *26*, 508.
(12) Komatsu, T. *J. Mater. Chem.* **2001**, *11*, 802.
(13) Jürgens, B.; Irran, E.; Senker, J.; Kroll, P.; Müller, H.; Schnick, W. *J. Am. Chem. Soc.* **2003**, *125*, 10288.
(14) Miller, D. R.; Wang, J.; Gillan, E. G. *J. Mater. Chem.* **2002**, *12*, 2463.
(15) Zimmerman, J. L.; Williams, R.; Khabashesku, V. N.; Margrave, J. L. *Russ. Chem. Bull.* **2001**, *50*, 2020.
(16) Mattesini, M.; Matar, S. F.; Etourneau, J. *J. Mater. Chem.* **2000**, *10*, 709.

10.1021/ic034984f CCC: $27.50 © 2004 American Chemical Society
Published on Web 01/06/2004

well as electronic properties of these materials is undisputable, synthetic approaches utilizing the knowledge of the formation processes and mechanistic pathways on the molecular level have largely been absent. The latter, however, might play a key role in overcoming hitherto unresolved questions concerning the structure of g-C_3N_4 phases and in devising and directing the formation of C_3N_4 solids in terms of systematic crystal engineering.

An appealingly simple synthetic route to extended carbon nitride networks is based on the thermal and high-pressure treatment of suitable C,N-containing molecules such as cyanamides and dicyanamides,[13] thiocyanates,[12] or melamine derivatives,[5,6,13,17] utilizing "self-condensation" reactions without the necessity of coreactants or specifically functionalized reaction sites. Although it is common practice to treat such thermal condensations as "black box" reactions, the elucidation of their mechanism and dynamic processes on the molecular level is a prerequisite to obtain well-defined solids with tailored connectivities.

In this contribution we report on the thermally induced solid-state reactivity of ammonium dicyanamide $NH_4[N(CN)_2]$ (NH_4dca), which was investigated using a range of diffraction and spectroscopic techniques. The crystal structure and temperature-dependent dynamics of $NH_4[N(CN)_2]$ as investigated by single-crystal X-ray as well as neutron powder diffraction, solid-state NMR, and vibrational spectroscopy have been treated elsewhere,[18] the results serving as a basis for the present discussion. Whereas, upon heating, the anions of alkali metal and alkaline earth metal dicyanamides undergo trimerization to tricyanomelaminates above 260 °C[19−21] and polymerization yielding X-ray amorphous products between 280 and 440 °C,[22] respectively, a unique solid−solid phase transition has been observed for $NH_4[N(CN)_2]$ (**1**).[23,24] The ionic compound isomerizes into molecular dicyandiamide $NCN{=}C(NH_2)_2$ [**2** (dda)] upon heating, which may be regarded as the analogue of Wöhler's historic conversion of ammonium cyanate into urea (Scheme 1).[25,26] An intriguing feature of the dca/dda system is its close relation to melamine which is formed when heating dicyandiamide above 170 °C and, hence, its suitability for the generation of graphitic carbon nitride phases. The potential of this reaction pathway has recently been demonstrated by the synthesis and full characterization of melem $C_6N_7(NH_2)_3$.[13]

Scheme 2 illustrates two feasible molecular mechanisms drawn in analogy to those familiar from solution chemistry.

Scheme 1. Transformation of $NH_4[N(CN)_2]$ (**1**) into the Isomeric $NCN{=}C(NH_2)_2$ (**2**)[a]

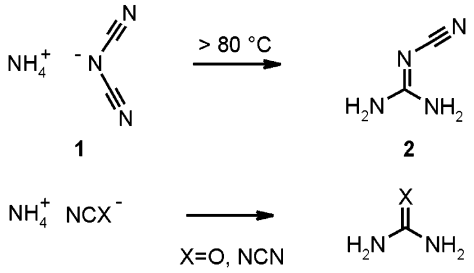

[a] The reaction represents the isolobal analogue of Wöhler's classic transformation of ammonium cyanate into urea.

The proposed reaction pathways particularly differ in terms of the initial proton transfer, which can proceed either to the bridging or to the terminal nitrogen atoms of the anion, thereby leading to the cyanoamine or cyanoimine tautomer of $NCN{=}C(NH_2)_2$ (Scheme 3). The subject of this paper will be the detailed discussion of this elementary solid-state reaction with respect to thermal, structural, and topological aspects as well as dynamical processes at the molecular level.

Experimental Section

1. Synthesis. $NH_4[N(CN)_2]$ was prepared by ion exchange in aqueous solution. An aqueous solution of NH_4Cl (Fluka, ≥98%, 1−2.5 M), corresponding to 3−7 times the theoretical exchange capacity, was given on a column containing an ion-exchange resin in strongly acidic form (Merck, Ionenaustauscher I, H^+ form, Art. 4765). The H^+/NH_4^+ exchange was considered to be complete when the pH of the eluate reached that of a saturated NH_4Cl solution (pH 4−5). Subsequently, the exchange resin was washed thoroughly with deionized water and the removal of excess chloride was substantiated using $AgNO_3$ as a precipitating agent. To provide the counterion, a solution containing $Na[N(CN)_2]$ (Fluka, ≥96%, 0.5 M) was poured onto the column and the eluate, which was evaporated at room temperature, gave colorless, needle-shaped crystals (yield ≈ 100%). The deuteration was effected by dissolving $NH_4[N(CN)_2]$ (3.0 g) in D_2O (Deutero GmbH, 99.9%, 20 mL) and stirring the colorless solution under argon at 40 °C for 1 h. After drying of the product in vacuo, the procedure was repeated twice and the white powdered product stored under argon.

2. Raman Spectroscopy. Variable-temperature Raman spectra were recorded on a Spectrum 2000 NIR−FT-Raman spectrometer (Perkin-Elmer) equipped with an integrated heating device and operating with a Nd:YAG laser optics system (λ = 1064 mm). Measurements were conducted between 100 and 115 °C in steps of 5 °C, the temperature being controlled by a Ni−Cr−Ni thermocouple. During the measurements, the sample (30 mg) was contained in a glass tube (diameter 2 mm) open to the atmosphere.

3. X-ray Diffraction. X-ray single-crystal diffraction data between 200 and 385 K were collected on a four-circle diffractometer (STOE Stadi 4) equipped with a 600 Series cryostream cooler (Oxford Cryosystems) using graphite-monochromated Mo Kα radiation (λ = 71.073 pm). The starting temperatures during variable-temperature measurements were adjusted by applying heating rates of 1 °C min^{-1}. The crystal structure was solved by direct methods using the SHELXS-97 program[27] and refined anisotropically for all non-hydrogen atoms by the least-squares method on F^2 using SHELXL-97.[28]

(17) Alves, I.; Demazeau, G.; Tanguy, B.; Weill, F. *Solid State Commun.* **1999**, *109*, 697.
(18) Lotsch, B. V.; Senker, J.; Kockelmann, W.; Schnick, W. *J. Solid State Chem.* **2003**, *176*, 180.
(19) Purdy, A. P.; House, E.; George, C. F. *Polyhedron* **1997**, *16*, 3671.
(20) Irran, E.; Jürgens, B.; Schnick, W. *Chem.−Eur. J.* **2001**, *7*, 5372.
(21) Jürgens, B.; Irran, E.; Schneider, J.; Schnick, W. *Inorg. Chem.* **2000**, *39*, 665.
(22) Jürgens, B.; Irran, E.; Schnick, W. *J. Solid State Chem.* **2001**, *157*, 241.
(23) Madelung, W.; Kern, E. *Liebigs Ann. Chem.* **1922**, *427*, 1.
(24) Jürgens, B.; Höppe, H. A.; Irran, E.; Schnick, W. *Inorg. Chem.* **2002**, *41*, 4849.
(25) Wöhler, F. *Ann. Phys. (Berlin)* **1828**, *12*, 253.
(26) Liebig, J.; Wöhler, F. *Ann. Phys. Leipzig, Ser. 2* **1830**, *20*, 369.
(27) Sheldrick, G. M. *SHELXS97, Program for the Solution of Crystal Structures*; University of Göttingen: Göttingen, Germany, 1997.

Scheme 2. Two Possible Reaction Pathways for the Isomerization of Ammonium Dicyanamide to Dicyandiamide in the Solid State, Based on the Two Mesomeric Forms of the Dicyandiamide Anion[a]

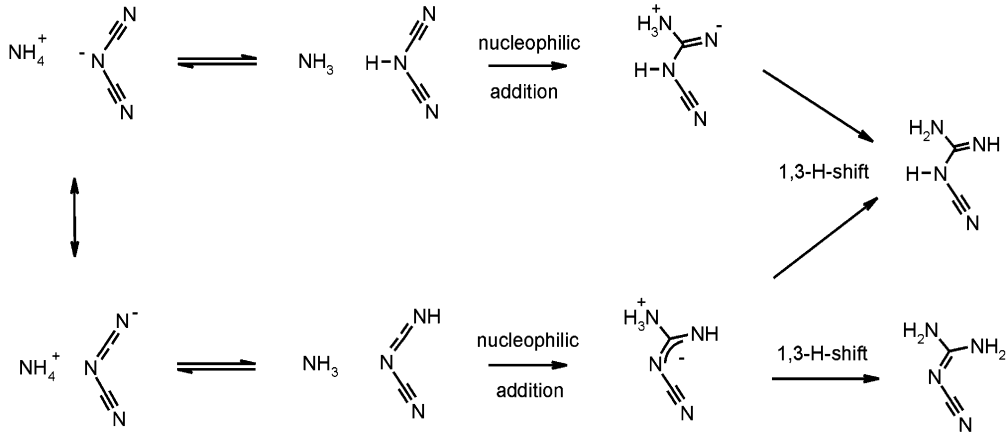

[a] Both reaction sequences are initiated by a proton transfer, followed by nucleophilic addition of the in situ generated ammonia forming a zwitterionic intermediate. From this stage, the cyanimino or cyanamino tautomers are generated via 1,3-H-shift.

Scheme 3. Tautomeric Structures of Dicyandiamide[a]

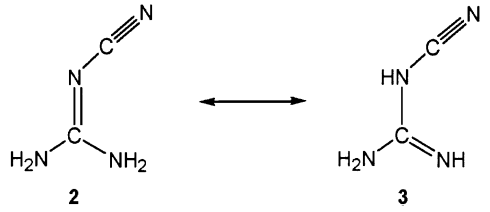

2 **3**

[a] Key: left, cyanoimine form **2**; right, cyanoamine form **3**.

Further details of the crystal structure determination are documented in a previous paper.[18]

High-temperature in situ X-ray diffractometry was performed on a STOE Stadi P powder diffractometer (Mo $K\alpha_1$ radiation, λ = 70.093 pm), with an integrated furnace and unsealed glass capillaries as sample containers from 85 to 105 °C. The data collection was restricted to a 2θ range of 11.5−13.5° and a single scan collection time of 3 min. The sample was heated to the starting temperature by applying a heating rate of 1 °C min^{-1}.

4. Neutron Powder Diffraction. Time-of-flight (TOF) neutron diffraction data for a deuterated sample of ammonium dicyanamide were collected on the ROTAX instrument at the ISIS spallation source of the Rutherford Appleton Laboratory, Chilton, Didcot, U.K.[29] The experimental procedure as well as technical details are reported elsewhere.[18] Powder diffraction patterns were recorded in a temperature range between 10 and 370 K at 13 different temperatures using a hot-stage closed cycle refrigerator[30] with a Eurotherm type 2408 temperature control (Eurotherm Controls Limited) equipped with Pt sensors (Pt100). The acquisition times varied between 30 min (high-temperature runs near the transformation onset) and 6 h, according to the temperature.

Information on the deuterium thermal behavior was extracted primarily from the high-resolution data ($\Delta d/d = 0.0035$, d = lattice spacing) obtained from bank 3 in backscattering geometry. The data for the three detector banks were refined simultaneously with the structure refinement program GSAS, which is based on the Rietveld method.[31,32] Anisotropic atomic displacement parameters were used for the deuterons and the ammonium-nitrogen atom from 10 to 365 K.

Further details of the neutron diffraction data may be found in the literature.[18]

5. Thermal Analysis. Thermoanalytical measurements between room temperature and 300 or 500 °C were recorded and analyzed on a Mettler DSC 25 with variable heating rates between 0.5 and 50 °C min^{-1}. For combined DTA/TG measurements between room temperature and 500 °C using heating rates of 1, 5, and 10 °C min^{-1} a Setaram thermoanalyzer TGA 92-2400 was available.

6. Solid-State NMR Spectroscopy. ^{13}C and ^{15}N CP-MAS-NMR spectra were measured on a DSX Avance 500 solid-state NMR spectrometer (Bruker, Karlsruhe, Germany) with two phase-sensitive detectors in quadrature in a temperature range between room temperature and 87 °C. The powdered sample was contained in a ZrO_2 rotor (diameter: 4 mm) which was sealed by a pierced *h*-BN cap for pressure equalization and placed in a double-resonance commercial MAS probe (Bruker, Karlsruhe, Germany). A sample of $Pb(NO_3)_2$, whose chemical shift exhibits a well-reproducible linear temperature dependence of +0.753 ppm K^{-1}, was used for calibration of the relative temperature at different spinning rates. The melting point of a benzile sample (95 °C) served as absolute temperature reference. The MAS spectra were recorded with an 8-step phase-cycled CP (cross-polarization) impulse sequence (contact times 10 ms (^{13}C) and 20 ms (^{15}N)) at 5 kHz (^{13}C) and 1.5 kHz (^{15}N) spinning frequency, respectively. The spinning frequencies were optimized with respect to the extraction of the isotropic and anisotropic properties of the chemical shift interaction by simulating and iteratively fitting the spectra using the NMR simulation software package Simpson.[33] The proton decoupling was effected by a TPPM (two pulse phase modulation) impulse sequence.[34]

Results

Thermal Analysis. DSC and DTA/TG measurements have been conducted to detect and characterize the thermal events accompanying the phase transition of $NH_4[N(CN)_2]$ to $NCN{=}C(NH_2)_2$. Within the investigated temperature range,

(28) Sheldrick, G. M. *SHELXL97, Program for the Refinement of Crystal Structures*; University of Göttingen: Göttingen, Germany, 1997.
(29) *ISIS Facility Annual Report*; 2001−2002; RAL-TR-2002-050.
(30) Bailey, I. F. *Z. Kristallogr.* **2003**, *218*, 84.
(31) Rietveld, H. M. *J. Appl. Crystallogr.* **1969**, *2*, 65.
(32) Larson, A. C.; von Dreele, R. B. *Programm GSAS General Structure Analysis System*; Los Alamos National Laboratory: Los Alamos, NM, 1994.
(33) Bak, M.; Rasmussen, J. T.; Nielsen, N. C. *J. Magn. Reson.* **2000**, *147*, 296.
(34) Bennett, A. E.; Rienstra, C. M.; Auger, M.; Lakshimi, K. V.; Griffin, R. G. *J. Chem. Phys.* **1995**, *103*, 6951.

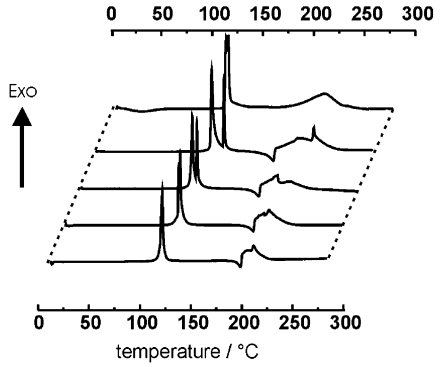

Figure 1. DSC curves showing the thermal behavior of $NH_4[N(CN)_2]$ between room temperature and 300 °C at heating rates 0.5, 1, 2, 5, and 7 °C min^{-1}. For better visualization, an *x*-axis offset of 8 °C for each curve was chosen.

a strongly exothermic signal is observed between 110 and 153 °C, depending on the heating rate, followed by a less exothermic signal around 200 °C and a weakly endothermic event between 330 and 360 °C. Whereas the first two signals can be attributed to the transformations of ammonium dicyanamide into dicyandiamide and dicyandiamide into melamine, respectively, the third event may indicate the melting process of melamine (mp 345 °C).[35] The cooling curves do not exhibit distinct features, which is indicative of an irreversible conversion of melamine into polymeric C−N−H products. This also holds for scans with a maximum temperature of 200 °C indicating the irreversibility of the observed NH_4dca → dda phase transition. Moreover, the transformation can be classified as "true" solid-state reaction owing to the absence of a premelting effect identifiable by an endothermic drop in the baseline prior to the onset of the exothermic signal (Figure 1). This observation, however, is only true for low heating rates (≤10 °C min^{-1}), whereas at high heating ramps an endothermic drift is detectable. Therefore, under conditions far beyond the thermodynamic equilibrium, the transformation loses its all solid-phase character. Accordingly, the enthalpy of the strongly exothermic transformation (value expected from calculations based on bond increments and neglecting lattice energetic effects: 26 kJ mol^{-1}) varies between 56 (0.5 °C min^{-1}) and 13 kJ mol^{-1} (50 °C min^{-1}), thereby again indicating potential changes in the transformation process (Table 1). A prominent feature of the DSC curves recorded at intermediate heating rates (1−6 °C min^{-1}) is the splitting of the strongly exothermic signal which reaches a maximum at about 5 °C min^{-1}. This observation might be rationalized by partial melting of the sample due to the heat generated by the highly exothermal character of the transformation *after* the onset of the reaction. This may cause a retardation resulting in a macroscopic two-step transformation process, where one part of the sample undergoes a solid−solid phase transition whereas the other part transforms starting from the melt. This interpretation is corroborated by the X-ray diffraction pattern of a sample recorded after interruption of the heating process just before the occurrence of the second split signal: it only exhibits broad reflections indicating poorly crystalline dda together with a high amorphous background.

Table 1. Results of the Thermoanalytical Measurements (DSC, DTA/TG) for $NH_4[N(CN)_2]$ (Room Temperature−300 °C), Including the Onset Temperature of the Transformation, Enthalpy Change, and Mass Loss Observed for the Different Heating Rates[a]

heating rate/ °C min^{-1}	*T*/°C	enthalpy/ kJ mol^{-1} (DSC)	mass loss/ % (TG)
0.5	**110**	56	
1	**117***	60	9.5
2	**122***	50	
3	126*	35	
4	125*	51	
5	**127***	52	7.7
6	130*	33	
7	**131**	22	
10	135	31	11.8
50	153	13	

[a] The DSC curves shown in Figure 1 are indicated by bold type. The asterisked onset temperatures refer to the first peak of the split signal; the corresponding enthalpies are the sums over both peaks.

Apparently, the splitting seems to be an interplay between the amount of heat generated during the transformation and the heating rate. It may be inferred from the relative peak heights and separation of the signals that only at intermediate heating rates this two-step process becomes evident, whereas at sufficiently slow and high ramps only the second and first peaks, respectively, are resolved. In first approximation, the splitting seems to be independent of the enthalpy change associated with the transformation at a particular heating rate. This fact may be explained by assuming the first signal to reflect the amount of heat generated, which in all cases may suffice to cause the proposed melting effect after the reaction onset, whereas the second peak is losing intensity with increasing heating rate. However, no definitive interpretation of these findings may be given as yet, and it is believed that macroscopic effects and artifacts due to the varying heating rates are likely to play the key roles in the observed splitting. A microscopic two-step reaction mechanism exhibiting two separable exothermic events, which necessitate a sufficiently stable intermediate seem to be rather unlikely.

Thermogravimetric DTA/TG measurements were carried out at heating rates of 1, 5, and 10 °C min^{-1}, the results of the DTA experiments being in close coincidence with those of the DSC measurements. By thermogravimetric measurements, a significant weight loss ranging between 9.5 (1 °C min^{-1}) and 11.8% (10 °C min^{-1}) accompanying the exothermic signal was detected, which is most probably due to the evolution of gaseous ammonia during the transformation. The total mass loss at 500 °C amounts to 33%. The "degasification" not only hints at the intermediate occurrence of free ammonia during the transformation but also indicates a growing tendency toward polymerization and amorphization of the starting material $NH_4[N(CN)_2]$. Therefore, an increasingly incomplete transformation into $NCN{=}C(NH_2)_2$ together with a change of the reaction mechanism must be assumed when raising the heating rate. This tendency is even more pronounced in open systems; if the reaction is carried out in closed vessels and the evolution of ammonia is accordingly counteracted, the transformation almost runs to completion.

(35) Lide, D. R., Ed. *Handbook of Chemistry and Physics*, 77th ed.; CRC Press: New York, 1997.

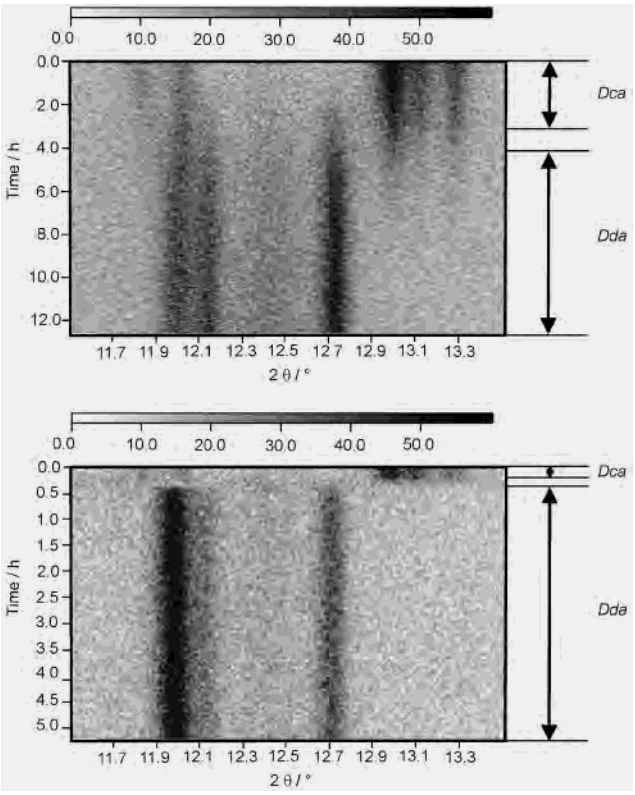

Figure 2. Temperature-dependent X-ray diffraction measurements at 90 °C (top) and 100 °C (bottom) between 11.5 and 13.5° in 2θ. To ensure a sufficiently small time window for the detection of structural changes and to simultaneously maintain an acceptable data quality, the data acquisition time for a single scan was fixed to 3 min. At 100 °C the phase transition is accompanied by an intermediate amorphous phase whereas at 90 °C the reflections of both reactants overlap.

In Situ X-ray Powder Diffraction. In situ powder diffraction data were collected in an angular 2θ range between 11.5 and 13.5° under isothermic conditions at 85, 90, 95, 100, and 105 °C. The sequences of X-ray powder patterns collected at 90 and 100 °C, respectively, are shown in Figure 2. A prominent feature of the variable-temperature studies is the absence of a unique onset temperature for the observed phase transition. Instead, the transformation onset is even observed at temperatures as low as 80 °C. However, at lower temperatures increasingly long induction periods and significantly reduced reaction rates are observed. Furthermore, the diffraction data collected at temperatures ≥100 °C consistently exhibit a transitory regime (3−6 min) where no reflections are detectable and, therefore, the occurrence of an amorphous phase or even intermediate melting must be inferred. Contrarily, at lower temperatures the coexistence of the starting and product phases is clearly distinguishable and no amorphous state is passed through. These findings demonstrate a significant dependence of the transformation process on the reaction conditions such as temperature, heating rate, pressure, etc.: at both higher heating rates when heating the sample from room temperature and at high starting temperatures, the transformation is increasingly accompanied by polymerization processes resulting in amorphous products. The strongly exothermic character of the transformation as well as its irreversibility and significant temperature dependence (variable transformation onset) also necessitate the question for the potential metastability of ammonium dicyanamide. The occurrence of the transformation can only be asserted for temperatures above 80 °C due to the long induction periods and slow transformation kinetics in this temperature range. However, it is still a point at issue whether ammonium dicyanamide is also thermodynamically unstable at temperatures below 80 °C, while being kinetically inert, or the transformation is favored thermodynamically only at temperatures above 80 °C.

Temperature-Dependent Single-Crystal X-ray Diffraction. Whereas the thermal and X-ray powder measurements are only suited to indicate rather macroscopic changes associated with the solid-state conversion of $NH_4[N(CN)_2]$ into $NCN{=}C(NH_2)_2$, variable-temperature single-crystal X-ray diffraction may be envisioned to be a powerful tool for the in situ tracing of structural changes prior to or, in convenient cases, even during the phase transition. The major drawback of this method, however, is its insensitivity to proton dynamics and transfer, the latter being a potential key step of the isomerization reaction. Thus, neutron diffraction measurements have additionally been conducted to direct the focus on the deuterium movement in the relevant temperature range.

Five complete single-crystal X-ray data sets were collected between 200 and 340 K. As a result, no major changes in the structural parameters and the *R*-values were observable. Above 340 K, only 14 characteristic reflections were scanned to reduce the data collection time in the critical temperature range. Surprisingly, instead of the expected total loss of the reflections due to the conversion of the single-crystal into polycrystalline material during the reaction, new relatively broad reflections occurred along with the broadening of the initial reflections. Upon basis transformation of the obtained unit cell into the conventional setting, the former turned out to be consistent with the metrics of the reaction product dicyandiamide dda ($C2/c$, $a = 1497.1(1)$, $b = 449.2(1)$, $c = 1310.6(1)$ pm, $\beta = 115.38(1)°$).[36]

To illustrate potential topological relations between the crystal structures of the starting material and the product, a line-up presentation of the actual orientations of the derived unit cells in the laboratory (goniometer) coordinate system is favorable. Therefore, the lattice parameters obtained from the orientation matrixes were visualized by a vector representation using the two separate nonorthogonal crystal coordinate systems of $NH_4[N(CN)_2]$ and $NCN{=}C(NH_2)_2$, respectively, with identical origin (Figure 3). The most eye-catching feature is the close coincidence between the spatial orientation of the crystallographic $a/-b'$ and $c/-a'$ axes, enclosing an angle of maximum 2°, respectively. Comparing the norm of the lattice vectors corroborates the initial trend in that one might roughly group the above pairs of axes into corresponding pairs of lattice parameters (a/b' 386(1)/449(2) pm, b/c' 1257(3)/1313(3) pm, $2c/a'$ 1810(3)/1497(5) pm).

(36) Hirshfield, F. L.; Hope, H. *Acta Crystallogr.* **1980**, *B36*, 406. The crystallographic data for dicyandiamide contained in the JCPDS database (SG *Pa*3, $a = 540.5$ pm) do not correlate in any way with the single-crystal data found in the literature and are therefore to be treated with caution. It is believed that they are based on an erroneous structure determination from powder diffraction data.

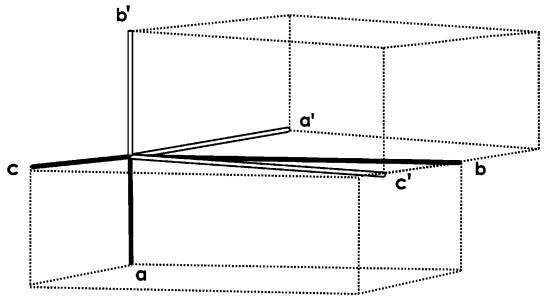

Figure 3. Representation of the lattice vectors of ammonium dicyanamide (black) and dicyandiamide (gray) as obtained from the orientation matrixes before (dca) and after (dda) the single-crystal to single-crystal transformation. The metric systems of the unit cells are illustrated by coordinate systems having the same origin.

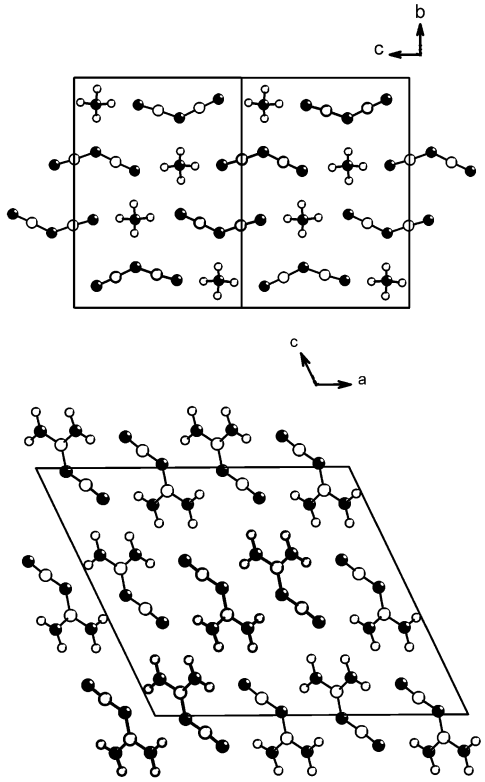

Figure 4. Top: Unit cell of ammonium dicyanamide with doubled *c* axis, viewed along [100]. Bottom: Unit cell of dicyandiamide, viewed along [0$\bar{1}$0]. The spatial orientation of the unit cells is based on the orientation matrixes of the single crystals and therefore illustrates the relative orientation of the reactants during the transformation. According to this representation, the reorientation of the molecules takes place in the molecular planes (paper plane) of the reactants.

In fact, by simultaneous visualization of the spatial orientation of the unit cells as obtained from the orientation matrixes, the molecular planes of the dca anions and dda molecules, respectively, are found to be oriented almost parallel in a plane perpendicular to that defined by the $a/-b'$ and $c/-a'$ axes (Figure 4). This preorientation significantly reduces the degrees of freedom necessary to directly correlate the positions of the dicyanamide ions with those of the product dda. Although the attempt to exactly identify corresponding atomic arrangements in the unit cells of dca and dda did not yield satisfactory results, it may be stated that according to the above findings the major degrees of freedom during the isomerization may be located in the molecular planes of both dca and dda molecules. The former may virtually be transferred into the latter by rotation around the inversion centers of the unit cell. Thus, a close topological relation between the metric systems of $NH_4[N(CN)_2]$ and $NCN{=}C(NH_2)_2$ must be inferred, which may justify the classification of the reaction at issue as a topochemical transformation.

Neutron Powder Diffraction. Neutron powder diffraction measurements using a deuterated sample of ammonium dicyanamide were conducted to elucidate both the dynamics of the ammonium group well below the phase transition and the deuteron transfer process in the transition temperature range, the former of which is treated elsewhere.[18]

An intriguing concept in the discussion of solid-state transformations comes into play when particular structural features of the starting component are potentially related to the product structure which is often valid in case of topochemical reactions. As discussed in the previous section, relations between the unit cell axes of $NH_4[N(CN)_2]$ and $NCN{=}C(NH_2)_2$ could be inferred. To go a step further, these findings may be correlated on the molecular level with the reaction processes at issue. By neutron diffraction the hydrogen positions could be reliably determined and the hydrogen-bonding network could therefore be readily characterized in a temperature range between 10 and 370 K. The four N−D distances and hydrogen bridges can be roughly divided into two pairs each, where the bond distances N4−D2/N4−D3 are longer on average than N4−D1/N4−D4, whereas, accordingly, the hydrogen bridges D2···N3/D3···N1 to the terminal (N1/N3) and bridging (N2) nitrogen atoms of the anion are systematically shorter than D1···N3/D4···N2: average D···N distances for D1 and D4 range between 195 and 217 pm (10 and 370 K); those for D2 and D3, between 185 and 199 pm (Figure 5).[18] This, however, is consistent with a more pronounced fixation of the deuterons along [001] (D2/D3) due to stronger hydrogen bonding to the anion. This tendency remains practically constant over the whole temperature range and is accompanied by a slight contraction of the *c* axis (−0.4%)[18] upon heating due to a negative coefficient of thermal expansion. These observations might be correlated with the findings from single-crystal X-ray diffraction, where the doubled *c* axis of $NH_4[N(CN)_2]$ is somewhat longer than the *a* axis of the product ($2c/a'$ 1810(3)/1497(5) pm). Presumably, the continuous contraction along *c* contributes to a preparatory positioning and orientation of the ions in the parent phase which may cause the phase transformation to proceed topochemically without any abrupt structural distortions.

The temperature factors of the deuterons were refined anisotropically at various temperatures to visualize librational and translational effects due to thermal movement and, hence, the trajectory of each deuteron.

The steady increase of the thermal displacement parameters with increasing temperature can be interpolated almost linearly for the deuterons D2, D3, and D4, whereas those of D1 rise nonlinearly (Figure 6). This disproportionate increase

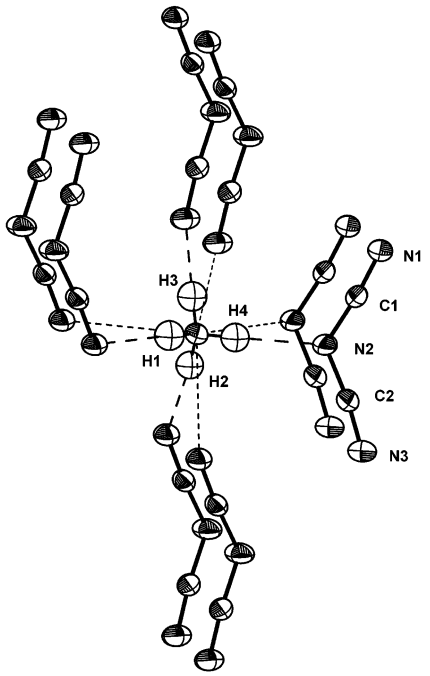

Figure 5. Coordination sphere and hydrogen bonding network of the ammonium ion in $NH_4[N(CN)_2]$. The central nitrogen of the ammonium group is labeled N4.

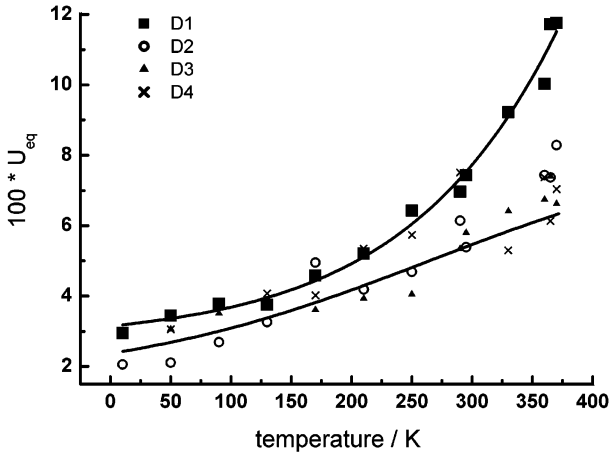

Figure 6. Temperature behavior of the thermal displacement parameters U_{eq} of the deuterium atoms of ND_4^+ between 10 and 370 K. U_{eq} is defined as one-third of the trace of the orthogonalized $\mathbf{U}_{ij}$ tensor. U_{eq} of D1 can be interpolated nonlinearly, whereas D2−D4 exhibit an almost linear temperature dependence. For clarity, the interpolation of data D2−D4 is represented by one single line. The error was estimated as $\pm 1 \times 100U_{eq}$.

may be indicative of the beginning detachment of D1 as a result of growing thermal vibrations. Since the distance to the adjacent nitrile nitrogen atom N3···D1 does not decrease accordingly with increasing temperature (see above), a directed deuteron transfer of D1 from N4 to N3 of the anion is questionable when based on the above findings alone. However, a "free" mobile proton (deuteron) must be considered to be the strongest acid possible and therefore to be not stable in the vicinity of basic centers. Since the adjacent nitrogen N3 of the anion is nearest, one can, nevertheless, on the basis of energetic considerations, assume the proton (deuteron) transfer to proceed to this nitrogen atom.

As reported previously,[18] Fourier cuts through the nuclear density of the ammonium group do not only illustrate the increasing smearing out of the probability density function (pdf) of the atoms with increasing temperature, which is especially pronounced for D1 and D4. There is also evidence for an ellipsoidal distortion of the N4 pdf along the direction of the bond N4−D1 from temperatures >295 K on, which may be indicative of an increasing thermal mobility of the center of gravity of ND_4^+ along this bond direction. The application of the TLS formalism[37] to the separation of librational and translational movements of the ND_4^+ group revealed that the thermal movement of the central nitrogen N4 is purely translational in nature, which can be rationalized by symmetry considerations for the center of mass (N4). Therefore, translational movement of the entire ammonium group can be identified with that of its center of gravity. Consequently, the shape of the N4 pdf at elevated temperatures may corroborate the thermally activated movement of the ND_4^+ group along the extension of the N4−D1 bond, which, together with the enlarged thermal ellipsoid of deuteron D1, might tentatively be interpreted in terms of the beginning detachment of D1 at the beginning of the solid−solid transformation.

Temperature-Dependent Raman Spectroscopy. Whereas structural changes can be probed by diffraction methods, vibrational spectroscopy is particularly sensitive to mechanistic details and dynamic processes on the local structural level, such as slight modifications of the hydrogen bridge network, proton transfer, etc. Since the $\nu_s(C{\equiv}N)$ and $\nu_{as}(C{\equiv}N)$ stretching vibrations of $NH_4[N(CN)_2]$ and $\nu_{as}(C{\equiv}N)$ of $NCN{=}C(NH_2)_2$ ($\nu_s(C{\equiv}N)$ is Raman inactive) appear as isolated, very intense bands in the Raman spectrum, the thermal evolution of these bands can clearly be distinguished. Spectra were recorded every 2 min at 100, 105, 110, and 115 °C. According to the literature, the doublet at 2158 and 2204 cm^{-1} in the product spectrum can be attributed to the cyanoimine and to the cyanoamine form of dicyandiamide, respectively (Scheme 3),[38,39] whereby the cyanoimine tautomer is prevailing in the solid state.[36,40−41]

In Figure 7, the high-frequency part of the spectrum is extracted, showing a succession of spectra recorded at constant temperatures (100 and 115 °C). The progression of the transformation is evidenced by the continuous decrease of the band intensity of the starting material at 2218 cm^{-1}. Whereas at lower temperatures the disappearance of $\nu_s(C{\equiv}N)$ ($NH_4[N(CN)_2]$) is accompanied almost instantly by the evolution of the product bands, indicating the coexistence of both phases, this does not hold for higher temperatures. At 115 °C the bands of the starting material almost disappear completely before the product bands become visible, being indicative of a glassy or molten intermediate with strongly

(37) Shomaker, W.; Trueblood, K. N. *Acta Crystallogr.* **1968**, *B24*, 63.
(38) Sheludyakova, L. A.; Sobolev, E. V.; Arbuznikov, A. V.; Burgina, E. B.; Kozhevina, L. I. *Faraday Trans.* **1997**, *93*, 1357.
(39) Alía, J. M.; Edwards, H. G. M.; García Navarro, F. J. *J. Mol. Struct.* **2001**, *597*, 49.
(40) Hughes, E. W. *J. Am. Chem. Soc.* **1940**, *62*, 1258.
(41) Jeremy-Jones, W.; Orville-Thomas, W. J. *Trans. Faraday Soc.* **1959**, *55*, 193.

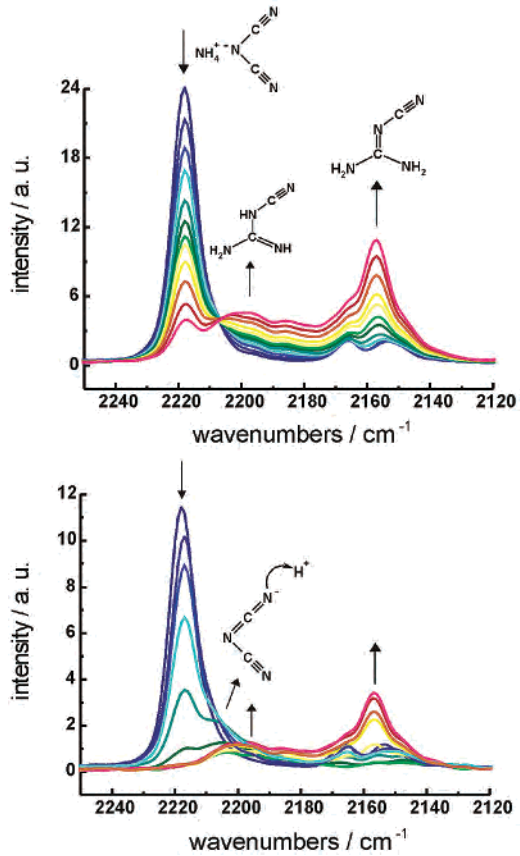

Figure 7. Sequence of Raman spectra of the nitrile stretching region recorded during the transformation in a frequency range of 2250−2120 cm^{-1}. The ν_s(C≡N) band of $NH_4[N(CN)_2]$ decreases continuously, whereas the nitrile stretching vibrations of the product tautomers steadily increase. Top: 100 °C. Bottom: 115 °C.

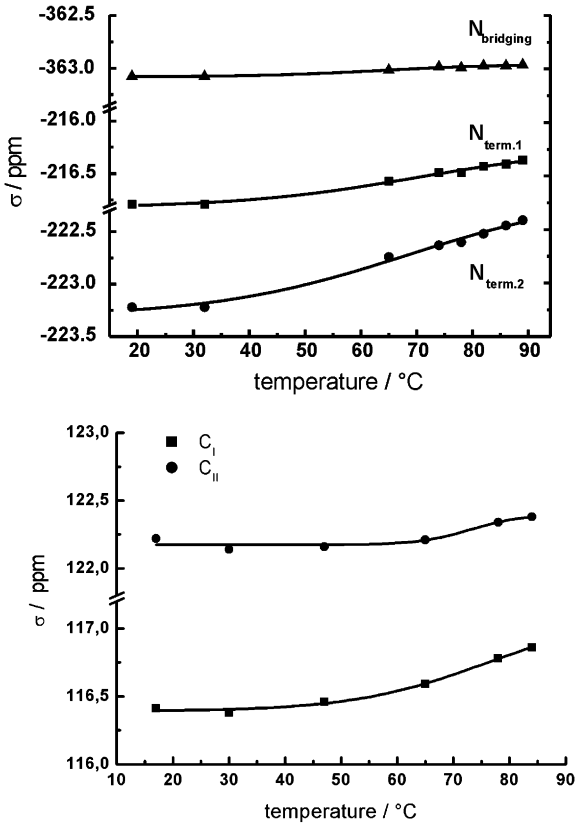

Figure 8. Temperature dependence of the isotropic chemical shift σ_{iso} in a temperature range from room temperature to 87 °C. Top: Isotropic chemical shifts of the three inequivalent ^{15}N nuclei of the dicyanamide anion, spinning rate 4.5−5 kHz. Bottom: Isotropic chemical shifts of the ^{13}C nuclei, spinning rate 5 kHz.

diminished scattering power. An interesting feature of this spectral region is the more rapid evolution of that part of the product doublet which can be attributed to the cyanoamine tautomer. This fact correlates well with the most plausible mechanistic pathway, in which the nucleophilic attack of the liberated ammonia at the electrophilic carbon atom leads to the cyanoamine form, giving the more stable cyanoimine isomer upon 1,3-H-shift. Another mechanistic implication may be obtained from the low-frequency side of the ν_s(C≡N) band of $NH_4[N(CN)_2]$. At higher temperatures a pronounced shoulder is visible around 2208 cm^{-1}, which cannot be identified with the stretching vibration of the cyanoamine tautomer. This red shift might, however, be interpreted in terms of a lowering of the ν_s(C≡N) stretching frequency of ammonium dicyanamide due to the reduction of the C≡N binding order at the nitrile group, thereby suggesting the onset of a proton transfer from the ammonium group to the terminal nitrogen. Upon protonation of the terminal nitrogen, still any of the two tautomers can be generated via 1,3-H-shift (Scheme 2). However, as it is evidenced by the respective band intensities, the cyanoimine tautomer is formed predominantly.

Thus, there seems to be strong evidence for the initial proton transfer to occur to one of the terminal nitrile nitrogen atoms and not, as could not be ruled out on the basis of the performed scattering experiments, to the central nitrogen of the dicyanamide anion.

^{13}C, ^{15}N MAS Solid-State NMR Investigations. Natural abundance ^{13}C and ^{15}N MAS NMR experiments were conducted in a temperature range between room temperature and 87 °C. By simulation of the obtained spectra using the software package Simpson,[33] all resonances could be assigned to the six ^{13}C and ^{15}N nuclei present in $NH_4[N(CN)_2]$.[18] As yet, the unequivocal assignment of the four resonances belonging to the crystallographically inequivalent carbon and nitrogen atoms of the nitrile group is still a point at issue. To clarify this question, ^{15}N- and ^{13}C-enriched samples together with coupling experiments are required. Until 77 °C, the spectra could be fitted iteratively without problems; however, since the onset of the transformation was accompanied by a significant loss of intensity, no data could be obtained for temperatures beyond 87 °C.

The temperature dependence of σ_{iso} for the nuclei ^{13}C and ^{15}N of the anion is illustrated in Figure 8. The temperature dependence of the spectral parameters for the ammonium nitrogen (^{15}N) is insignificant and has therefore not been included in the discussion. For all nuclei a uniform increase of the chemical shift interaction is evident, which is roughly within the same order of magnitude for both ^{13}C atoms. Contrarily, upon heating a differentiation of the three magnetically inequivalent nitrogen nuclei is clearly distinguishable. Whereas the chemical shift of the central nitrogen

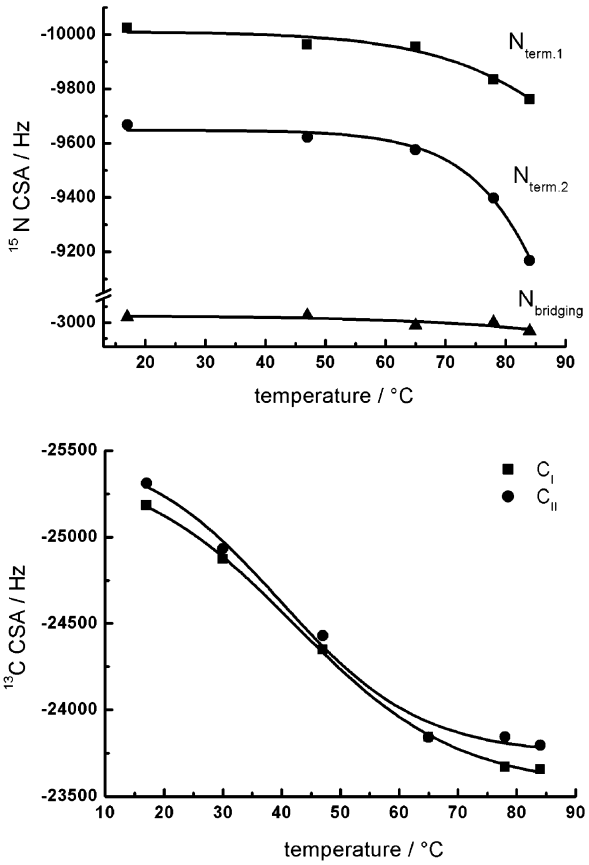

Figure 9. Temperature dependence of the chemical shift anisotropy CSA in a temperature range from room temperature to 87 °C. Top: ^{15}N, spinning rate 1.5 kHz. Bottom: ^{13}C, spinning rate 5 kHz.

does not change significantly, the terminal nitrogen atoms exhibit shifts $\Delta\sigma$ up to 1 ppm. Furthermore, the increase is more pronounced for one of the two terminal nitrogen atoms ($N_{term.2}$), indicating a differentiation in the respective electronic environments. Since the absolute changes are rather small compared to chemical shift differences due to hybridization effects, one can at best infer an incipient polarization of a nitrile nitrogen atom. This might be correlated with the beginning proton transfer from the ammonium ion to the terminal nitrogen which is expected to be accompanied by pronounced electronic deshielding of the latter. The strengthening of the hydrogen-bonding network which might have the same impact on the chemical shift changes can largely be excluded on the basis of the results from temperature-dependent neutron powder diffraction.[18]

The temperature dependence of the chemical shift anisotropy (CSA) of the ^{13}C and ^{15}N nuclei is shown in Figure 9. Again, the nitrile groups seem to be the "reactive centers", since all significant changes of the CSAs are predominantly associated with the carbon and terminal nitrogen atoms, whereas the bridging nitrogen again suffers minimal changes only. For all atoms of the nitrile group, a decrease in the CSA in the order of 5−6% is observed, which may be rationalized by two mechanisms presumably operating simultaneously: First, a decrease in anisotropy of the magnetic susceptibility may be a consequence of the increasing mobility of the nitrile groups without major changes of the molecular geometry at higher temperatures. A second factor may be the decrease in local electron density which effects a lowering of the polarizability of the C≡N bond and, hence, of the CSA.

By analogy with the chemical shift data, the CSA of $N_{term.2}$ falls off more rapidly than that of $N_{term.1}$, which suggests the major electronic changes to occur at one particular terminal nitrogen atom. As found for the ^{13}C chemical shift data, the commencing differentiation of the CSA at temperatures beyond 67 °C is not large enough to be correlated unambiguously with well defined changes in the crystallographic or electronic structure.

The asymmetry of the chemical shift tensor can only be judged with difficulties owing to complications in the profile fits due to the diminished intensity of the high-temperature data. As a general trend, the asymmetry of the bridging nitrogen atom as well as the carbon atoms and $N_{term.2}$ slightly increases ($\eta_{Nbridging} = 0.40 \rightarrow 0.57$, $\eta_{C1} = 0.22 \rightarrow 0.24$, $\eta_{C2} = 0.21 \rightarrow 0.25$), whereas that of $N_{term.1}$ slightly decreases ($\eta_{Nterm.1} = 0.23 \rightarrow 0.16$). Since for a proton transfer to a terminal nitrogen prior to the attack of a nucleophile the axial symmetry of the nitrile group is likely to undergo no major changes, the above findings are principally in line with the mechanism sketched above.

On the whole, since data of reasonable quality could only be obtained for temperatures slightly below the phase transition, the effects observed are necessarily small but may be assessed as to point in the same direction as those associated directly with the transformation.

Discussion

To provide a more general access to the solid state reaction outlined above, the most important findings of the various analytical methods applied will synoptically be surveyed in brief.

Upon heating under moderate conditions (heating rates ≤ 10 °C min^{-1}), the ionic ammonium dicyanamide undergoes a monotropic and strongly exothermic phase transition to the isomeric molecular dicyandiamide in a true solid-state reaction (Scheme 1). The transformation is most efficient in closed systems where the release of gaseous ammonia is counteracted. When the heating rates are increased, an increasing tendency toward polymerization and amorphization accompanied by drastically reduced reaction enthalpies is observed, which may indicate a change in the reaction mechanism. Presumably, a well-defined reaction pathway as sketched below (Scheme 2) is only valid for low heating rates or isothermal treatment of NH_4dca.

According to temperature-dependent single-crystal X-ray diffraction measurements, the reaction proceeds topochemically, resulting in a single-crystal to single-crystal transformation. From the orientation matrixes in the goniometer coordinate system, relations between corresponding axes of the unit cells could be derived and the molecular planes of the reactants associated with the major degrees of freedom necessary for the dicyanamide molecular ions to react. The hydrogen-bonding network surrounding the ammonium ion was characterized by neutron powder diffraction. The cation was found to be anisotropically fixed along [001] by two

pairs of unequally strong hydrogen bridges which may support the contraction of the *c* axis of $NH_4[N(CN)_2]$, serving for the adaptation of the corresponding axes $c/-a'$ of $NH_4[N(CN)_2]$ and $NCN{=}C(NH_2)_2$, respectively. An insight into the mechanism of the reaction is provided by temperature-dependent Raman and solid-state NMR spectroscopy. Both techniques give evidence for an initial proton transfer to one of the terminal nitrogen atoms of the dicyanamide ion. Neutron diffraction measurements reveal a disproportionately high increase of the thermal displacement parameter of D1 compared to the other deuterons. This may tentatively be associated with the commencing detachment of D1 and transfer to the nearest basic center, the terminal nitrogen N3 of an adjacent anion. Both the evolution of ammonia as evidenced by thermogravimetric measurements and the succession of the $\nu(C{\equiv}N)$ bands associated with the two tautomers of the product as detected by temperature-dependent Raman spectroscopy suggest a nucleophilic attack of ammonia at the electrophilic carbon of a nitrile group as is familiar from solution chemistry to be valid in the solid state as well.

Conclusion

An isolobal analogue to Wöhler's historic synthesis of urea, namely the transformation of $NH_4[N(CN)_2]$ into $NCN{=}C(NH_2)_2$, has been investigated using various diffraction and spectroscopic techniques. The mechanism that could be drawn illustrates the potential of solid-state reactions proceeding in an ordered and predictable manner. By analogy with solution chemistry, solid-phase transformations may be envisioned that can be devised and directed to selectively build up extended C−N networks under mild thermal conditions. This pathway may be particularly attractive for two-component or self-condensation reactions of simple triazine precursors such as cyanamides and dicyanamides or triazine derivatives, leading to highly condensed triazine-based systems such as melem, melam, or melon.[5,11−13]

Acknowledgment. The authors thank Dr. H. A. Höppe for the single-crystal data collection and Dipl. Chem. S. Correll for performing the temperature-dependent powder diffraction measurements as well as W. Wünschheim and Dipl. Min. S. Schmid for conducting the DSC and DTA/TG measurements. The authors are indebted to Dr. W. Kockelmann for his assistance at the neutron diffraction measurements at ISIS, which were supported by the Mineralogical-Petrological Institute of Bonn University and the BMBF (Contract 03KLE8BN); financial support was granted from the Fonds der Chemischen Industrie and the BMBF (scholarship for B.V.L.), which is gratefully acknowledged.

Supporting Information Available: Crystallographic information files (CIF) for $NH_4[N(CN)_2]$ at 200 K (single-crystal structure solution and refinement) and for $ND_4[N(CN)_2]$ at 10 K (Rietveld refinement of neutron powder data). This material is available free of charge via the Internet at http://pubs.acs.org.

IC034984F